

Supporting Information

Substantially enhanced front illumination photocurrent in porous SnO₂ nanorods / networked BiVO₄ heterojunction photoanode

Swetha S. M. Bhat, Jun Min Suh, Seokhoon Choi, Seung-Pyo Hong, Sol A Lee, Changyeon Kim, Cheon Woo Moon, Mi Gyoung Lee and Ho Won Jang *

Department of Materials Science and Engineering, Research Institute of Advanced Materials,
Seoul National University, Seoul 08826, Republic of Korea

*corresponding author email: hwjang@snu.ac.kr

Experimental Details

Synthesis of SnO₂ NRs/BVO: The photoanode SnO₂/BVO has been fabricated by a combination of glancing angle e beam deposition of SnO₂ nanorods and subsequent metal organic decomposition to grow BiVO₄ core shell on the SnO₂ nanorods. The length of the SnO₂ nanorods varied from 1-2 μm. GLAD method using e-beam evaporator was utilized to fabricate SnO₂ NRs on FTO/glass. SnO₂ grains with 99% purity (Kojundo Chemistry) was placed 50 cm below the substrate, which was tilted to 80° and rotated in speed of 80 rpm. The base pressure of the chamber was maintained at 1×10^{-6} Torr and the growth rate was 1.0 Å/s. After deposition of SnO₂ nanorods, all the fabricated samples were annealed at 550 °C for 2 h in air condition. Detailed procedure can be found in our previous works.^{1,2} Drop casting solution for BiVO₄ consists of (0.243 g) Bi(NO₃)₃·5H₂O and (0.123 g) VO((C₅H₇O₂)₂) which were dissolved in acetic acid and acetyl acetone with the ratio 20:1. The dark green solution was stirred for 1 h to get a transparent solution. Prior to the drop casting of the precursor solution, SnO₂ nanorods were soaked in acetic acid for 15 min to improve the wettability of the sample. Two drops of the 5 μl were drop casted on the SnO₂ nanorods and followed by heating in air at 350 °C on a hot plate for two minutes. Each layer consists of 2 drop casting and intermitted heating which is represented as nx where n is the number of layers. The fabricated heterojunction photoelectrodes were annealed in the furnace at 550°C for 3 h in air.

Photoelectrodeposition of cobalt phosphate (Co-Pi) has been carried out according to the published article by Nocera et al. Three electrode configuration was used for the photoelectrodeposition of Co-Pi. Pt plate as a counter electrode, Ag/AgCl as a reference electrode and SnO₂/BVO as working electrode with electrolyte of 0.5 mM of Co(NO₃)₃·6H₂O in 0.1 M potassium phosphate buffer (pH 7). The photodeposition was carried out at 0.6 V vs RHE for 200 s by Ivium potentiostat under the illumination corresponding to 1.5 G solar spectrum.

Materials Characterization: The phase of the samples was confirmed by Bruker D8 advance diffractometer equipped with Cu Kα source. The morphology of the SnO₂ NRs/BVO phototoanodes were characterized using a field-emission SEM (SU-70, Hitachi), with an acceleration voltage of 5 kV and working distance of 8 mm by field emission SEM (SU-Hitachi). The transmission electron microscope (TEM, JEOL, JEM-2100F) analysis were carried out at an accelerating voltage of 200 kV, which was equipped with high-angle annular dark-field image (HADDF), scanning TEM (STEM), and energy dispersive spectroscopy (EDS). UV-Visible absorbance spectra were obtained by JASCO UV-vis spectrometer. Gas chromatography measurement system (Agilent GC 7890B), which is equipped with a thermal conductivity detector and a micropacked column (ShinCarbon ST 100/120) was used to measure the O₂ evolution.

Photoelectrochemical characterization: Photoelectrochemical performances of SnO₂ NRs/BVO phototoanodes were measured with a typical three electrode configuration using Ivium potentiostat with

Ag/AgCl as reference electrode and Pt plate as a counter electrode. A 0.5 M Na₂SO₃ electrolyte with phosphate buffer solution was used as electrolyte for all the measurements. The light intensity solar simulator with an AM 1.5 G filter was calibrated to 1 sun (100 mW/cm²) using a reference cell. LSV measurement was carried out by sweeping in the anodic direction with scan rate of 20 mV/S. IPCE values were measured at 1.23 V vs. RHE using light source with monochromator. EIS was conducted at 1.23 V vs. RHE with the frequency range 10 mHz - 1000Hz and the obtained plots were fitted using ZSimpWin suite.

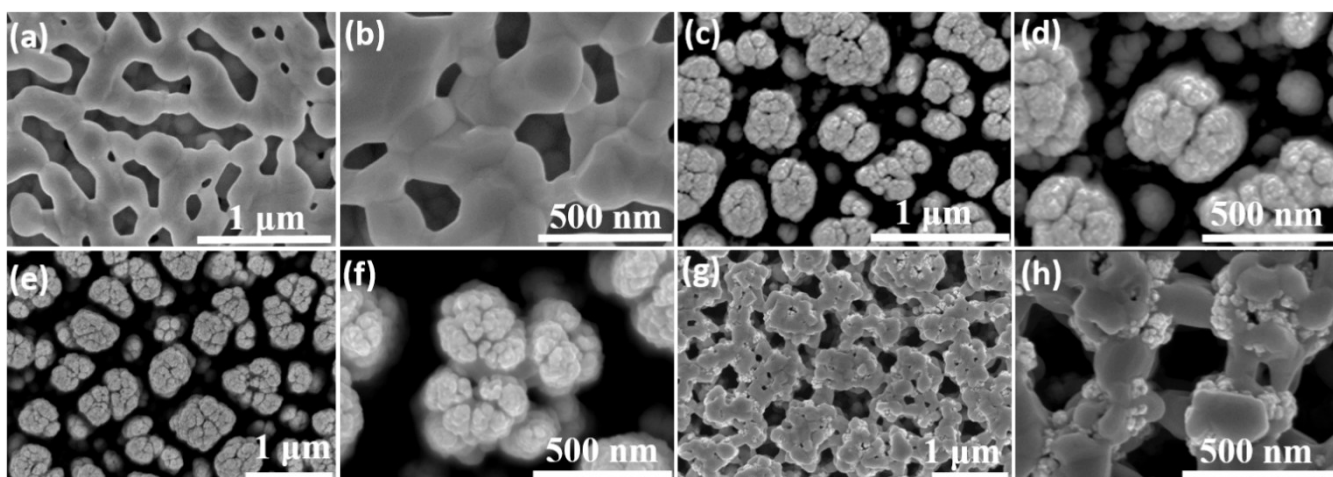


Figure S1. Scanning electron microscopy (SEM) top images of 1 μm SnO_2 NRs/BVO on FTO substrate at (a) low and (b) high magnification. SEM cross-section images of SnO_2 NRs/BVO on FTO substrate at (c) low and (d) high magnification. SEM top images of 2 μm SnO_2 NRs/BVO on FTO (a) (a) low and (b) high magnification. SEM cross-section images of SnO_2 NRs/BVO on FTO substrate at (c) low and (d) high magnification.

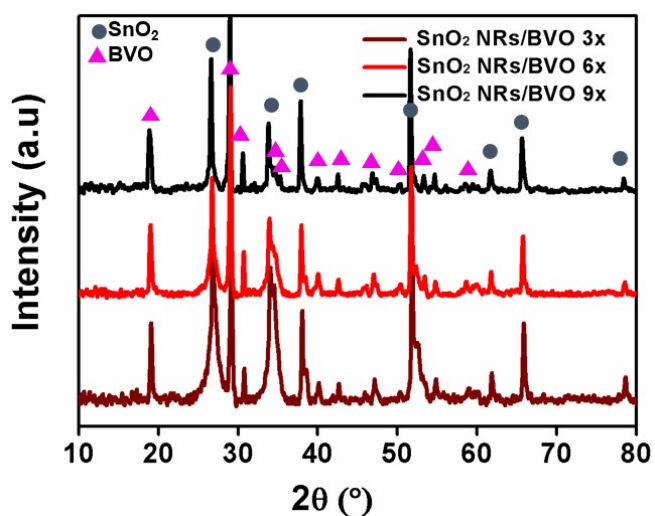


Figure S2. X-ray diffraction patterns of SnO_2 NRs/BVO at different layers of BiVO_4 .

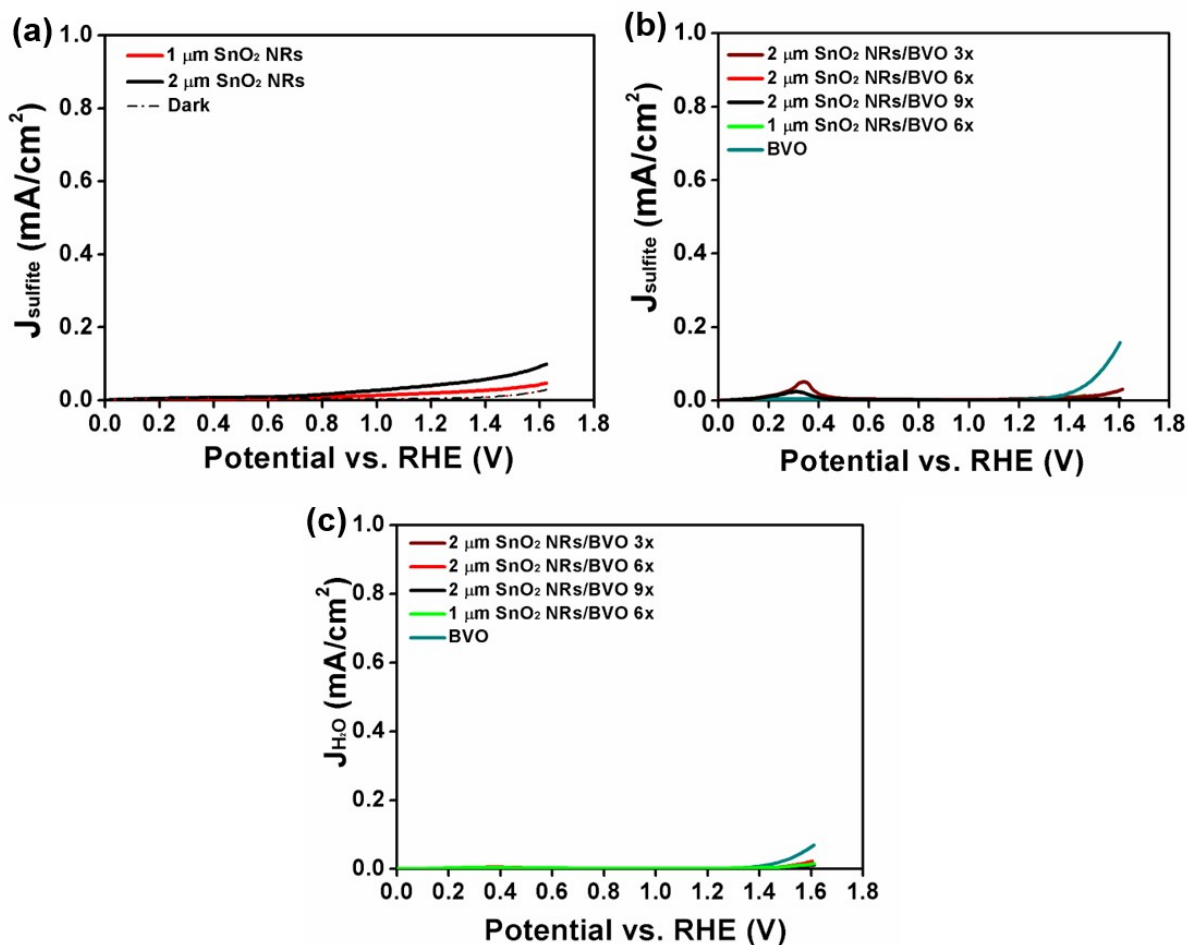


Figure S3. (a) LSV of pristine 1 μm and 2 μm SnO₂ NRs in aqueous phosphate buffer (pH 7.0) with 0.5 M Na₂SO₃ (b) LSV of SnO₂ NRs/BVO under dark in presence of aqueous phosphate buffer (pH 7.0) with 0.5 M Na₂SO₃ (c) LSV of SnO₂ NRs/BVO under dark in presence of aqueous phosphate buffer (pH 7.0) with 0.5 M Na₂SO₄.

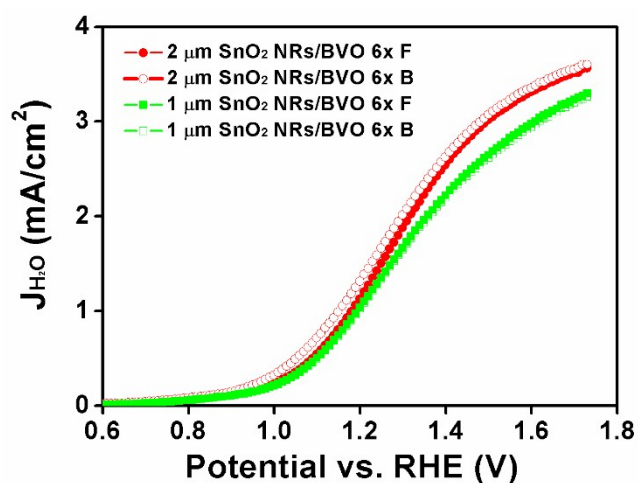


Figure S4. LSV of pristine 1 μm and 2 μm SnO₂ NRs/BVO in presence of aqueous phosphate buffer (pH 7.0) with 0.5 M Na₂SO₄.

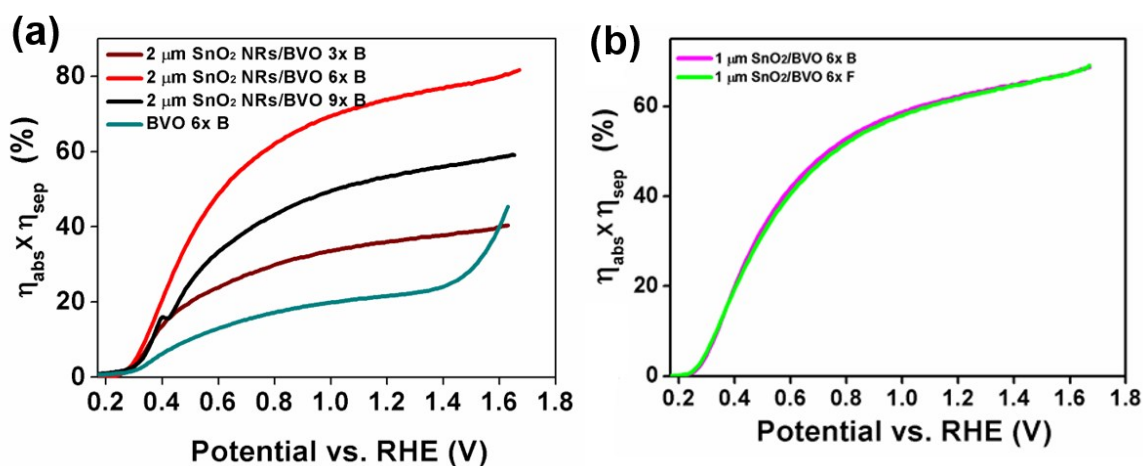


Figure S5. Charge separation efficiency of (a) 2 μm SnO₂ NRs/BVO photoanode under back illumination and (b) 1 μm SnO₂/BVO photoanode under back and front illumination.

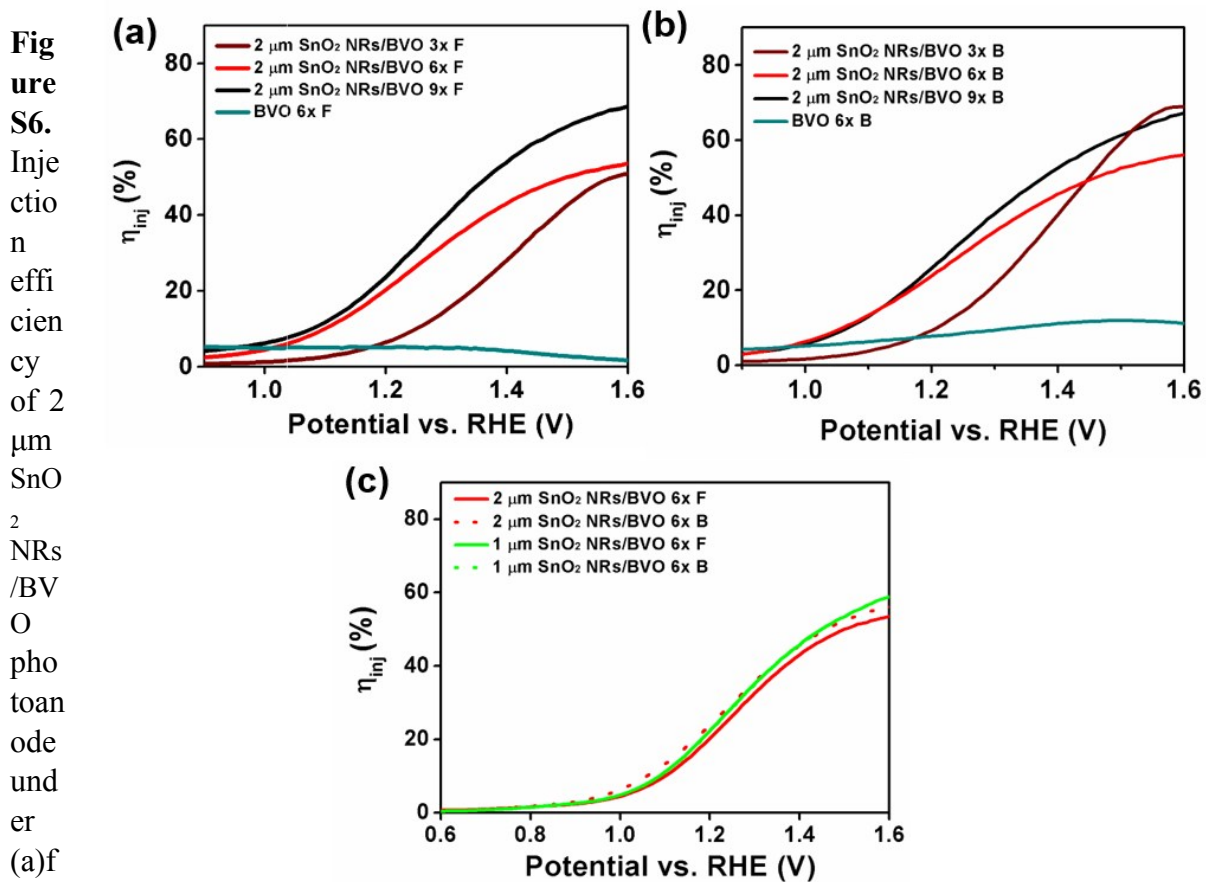
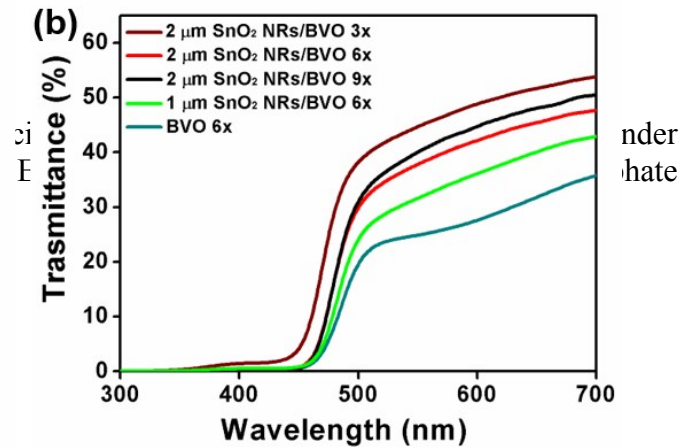
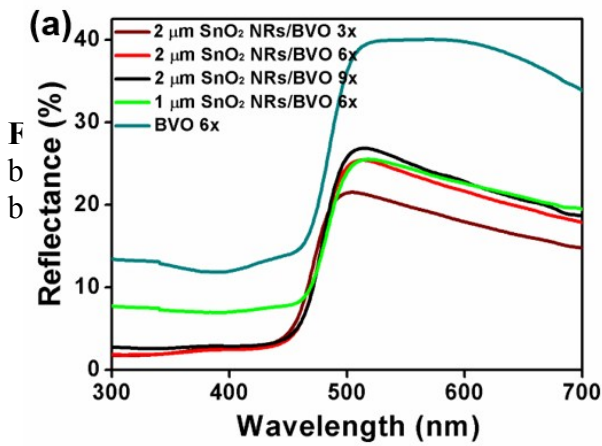
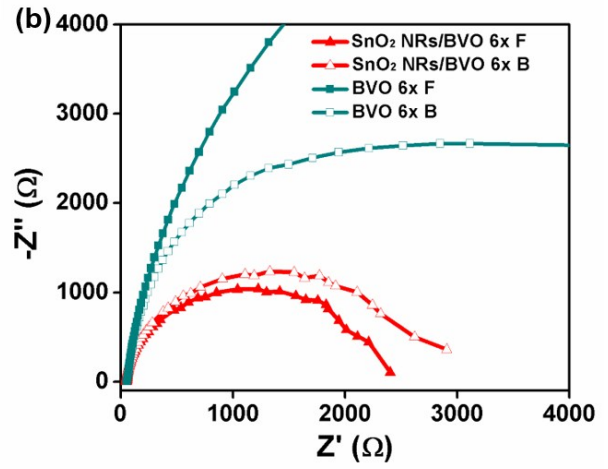
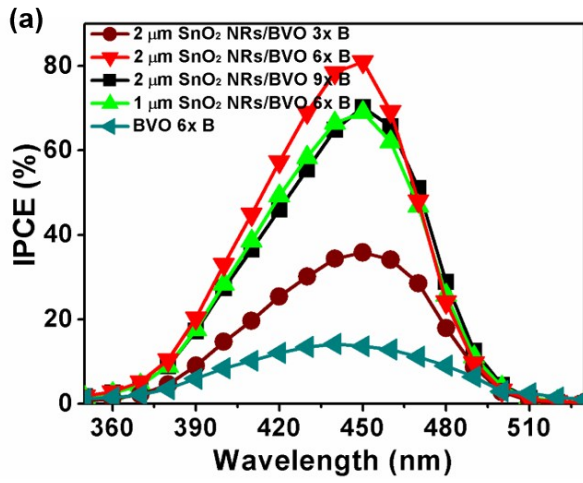


Figure S6. Injection efficiency of 2 μm SnO₂ NRs/BVO photoanode under (a) front illumination (b) back illumination and (c) 1 μm SnO₂ NRs/BVO photoanode under back and front illumination.



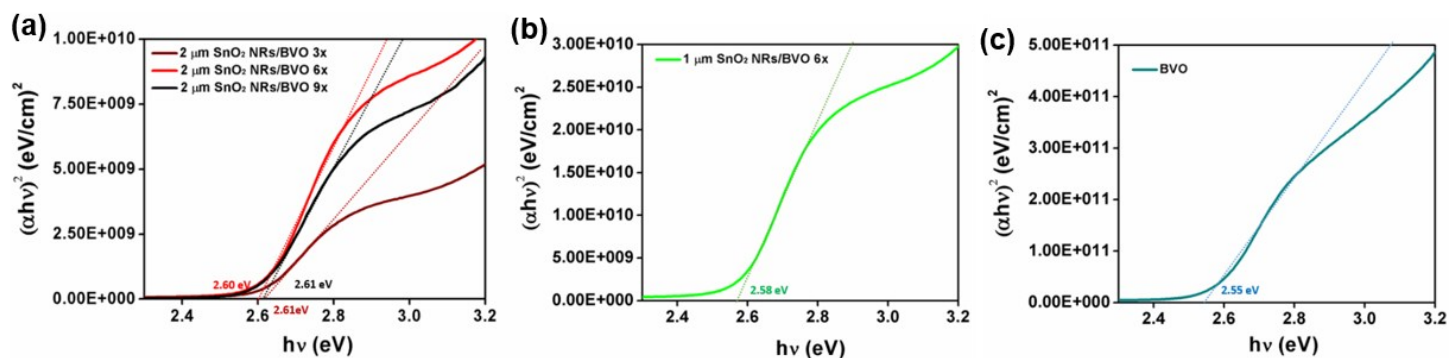


Figure S9. Tauc plots for (a) 2 μm SnO_2 NRs/BVO 3x, 6x and 9x, (b) 1 μm SnO_2 NRs/BVO, and (c) BiVO_4 .

Table S1. Flat band potential and donor density for SnO_2 NRs/BVO photoanodes.

Samples	Flat band potential	Donor density (Nd/cm^3)
2 μm SnO_2 NRs/BVO 3x	0.0611 V	2.15×10^{21}
2 μm SnO_2 NRs/BVO 6x	0.0527 V	3.61×10^{21}
2 μm SnO_2 NRs/BVO 9x	0.0959 V	1.78×10^{21}
1 μm SnO_2 NRs/BVO 6x	0.0647 V	0.91×10^{21}
BiVO_4	0.199 V	0.03×10^{19}

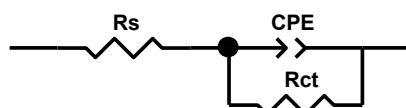


Figure S10. Equivalent circuit model of Nyquist plot.

Table S2.
results for various
NRs/BVO

Samples	R_s (Ω)	R_{ct} (Ω)
BiVO ₄	51.94	6631
2 μm SnO ₂ NRs/BVO 3x	56.54	3430
2 μm SnO ₂ NRs/BVO 6x	48.51	2350
2 μm SnO ₂ NRs/BVO 9x	57.86	4898
1 μm SnO ₂ NRs/BVO 6x	57.41	5590

Nyquist plot fitted
samples of SnO₂
photoanodes.

Table S3. Nyquist plot fitted results for various samples of SnO₂ NRs/BVO photoanodes.

Samples	R_s	R_{ct}
2 μm SnO ₂ NRs/BVO 6x F	48.51	2350
2 μm SnO ₂ NRs/BVO 6x B	49.42	2694

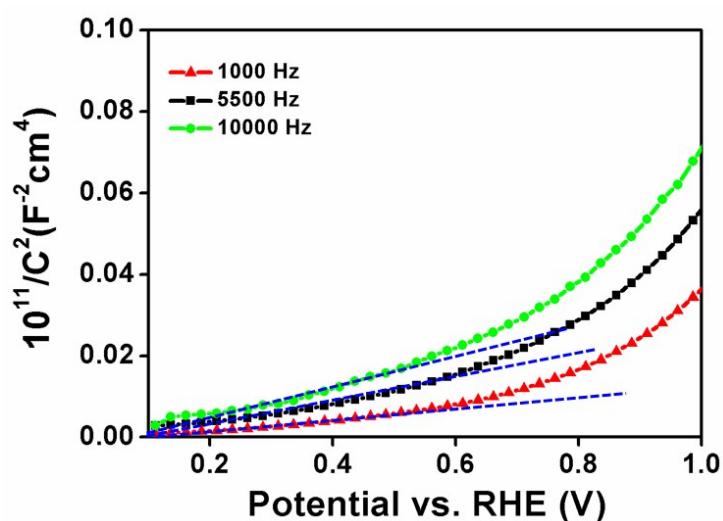


Figure S11. Mott-Schottky curves for SnO₂ NRs/BVO 6x at different frequencies.

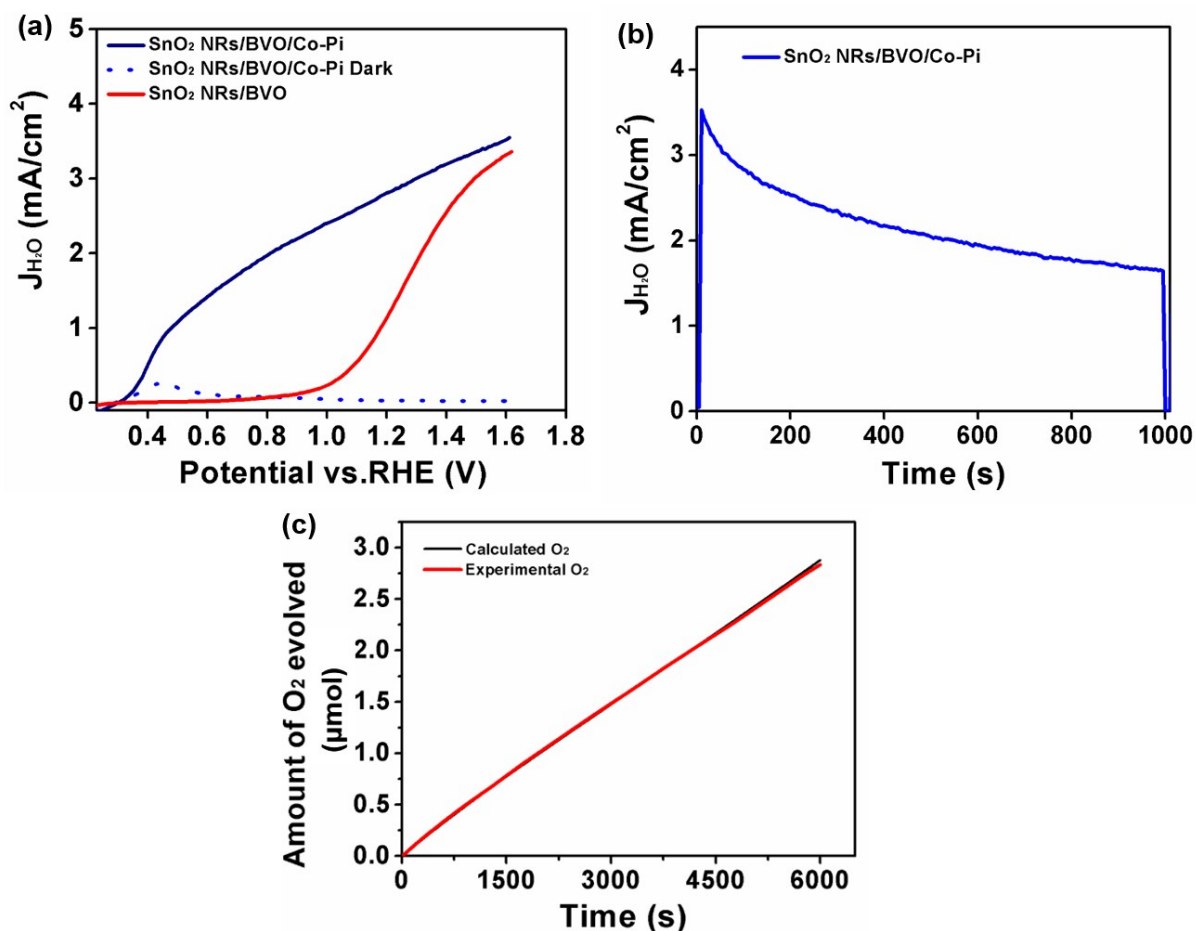


Figure S12. (a) LSV of SnO₂ NRs/BVO/Co-Pi (b) Stability measurement of SnO₂ NRs/BiVO₄ photoanode at 1.23 V vs. RHE (c) Oxygen evolution curves for SnO₂ NRs/BVO 6x at 1.23 V vs. RHE. All the above measurements were carried out in aqueous phosphate buffer (pH 7.0) with 0.5 M Na₂SO₄ under simulated solar illumination.

References

- 1 J. M. Suh, Y. S. Shim, D. H. Kim, W. Sohn, Y. Jung, S. Y. Lee, S. Choi, Y. H. Kim, J. M. Jeon, K. Hong, K. C. Kwon, S. Y. Park, C. Kim, J. H. Lee, C. Y. Kang and H. W. Jang, *Adv. Mater. Technol.*, 2017, **2**, 1–10.
- 2 J. M. Suh, W. Sohn, Y.-S. Shim, J.-S. Choi, Y. G. Song, T. L. Kim, J.-M. Jeon, K. C. Kwon, K. S. Choi, C.-Y. Kang, H.-G. Byun and H. W. Jang, *ACS Appl. Mater. Interfaces*, , DOI:10.1021/acsami.7b14545.